IOPscience iopscience.iop.org

Home Search Collections Journals About Contact us My IOPscience

Investigation of a novel material for magnetoelectronics: $Co_2Cr_{0.6}Fe_{0.4}Al$

This article has been downloaded from IOPscience. Please scroll down to see the full text article.

2003 J. Phys.: Condens. Matter 15 7019

(http://iopscience.iop.org/0953-8984/15/41/010)

View the table of contents for this issue, or go to the journal homepage for more

Download details:
IP Address: 171.66.16.125
The article was downloaded on 19/05/2010 at 15:20

Please note that terms and conditions apply.

INSTITUTE OF PHYSICS PUBLISHING JOURNAL OF PHYSICS: CONDENSED MATTER

J. Phys.: Condens. Matter **15** (2003) 7019–7027 PII: S0953-8984(03)67522-3

Investigation of a novel material for magnetoelectronics: $Co_2Cr_{0.6}Fe_{0.4}Al$

C Felser[1,5], B Heitkamp[2], F Kronast[2], D Schmitz[3], S Cramm[4], H A Dürr[2], H-J Elmers[1], G H Fecher[1], S Wurmehl[1], T Block[1], D Valdaitsev[1], S A Nepijko[1], A Gloskovskii[1], G Jakob[1], G Schönhense[1] and W Eberhardt[2]

[1] Johannes Gutenberg-Universität Mainz, 55099 Mainz, Germany
[2] BESSY GmbH, Albert-Einstein-Straße 15, 12489 Berlin, Germany
[3] Hahn-Meitner-Institut Berlin GmbH, Glienicker Straße 100, 14109 Berlin, Germany
[4] Forschungszentrum Jülich GmbH, IFF, 52425 Jülich, Germany

E-mail: felser@uni-mainz.de

Received 7 August 2003
Published 3 October 2003
Online at stacks.iop.org/JPhysCM/15/7019

Abstract

Heusler compounds are promising candidates for future spintronics device applications. The electronic and magnetic properties of $Co_2Cr_{0.6}Fe_{0.4}Al$, an electron-doped derivative of Co_2CrAl, are investigated using circularly polarized synchrotron radiation and photoemission electron microscopy (PEEM). Element specific imaging reveals needle shaped Cr rich phases in a homogeneous bulk of the Heusler compound. The ferromagnetic domain structure is investigated on an element-resolved basis using x-ray magnetic circular dichroism (XMCD) contrast in PEEM. The structure is characterized by micrometre-size domains with a superimposed fine ripple structure; the lateral resolution in these images is about 100 nm. The domains look identical for Co and Fe giving evidence of a ferromagnetic coupling of these elements. No ferromagnetic contrast is observed at the Cr line. Magnetic spectroscopy exploiting XMCD reveals that the lack of magnetic moment, detected in a SQUID magnetometer, is mainly due to the moment of the Cr atom.

(Some figures in this article are in colour only in the electronic version)

1. Introduction

Materials which display large changes in resistivity in response to an applied magnetic field (magnetoresistance) are currently attracting great interest due to their potential for applications in magnetic sensors, magnetic random access memories and spintronics [1]. The precondition

[5] Author to whom any correspondence should be addressed.

 © 2003 IOP Publishing Ltd Printed in the UK

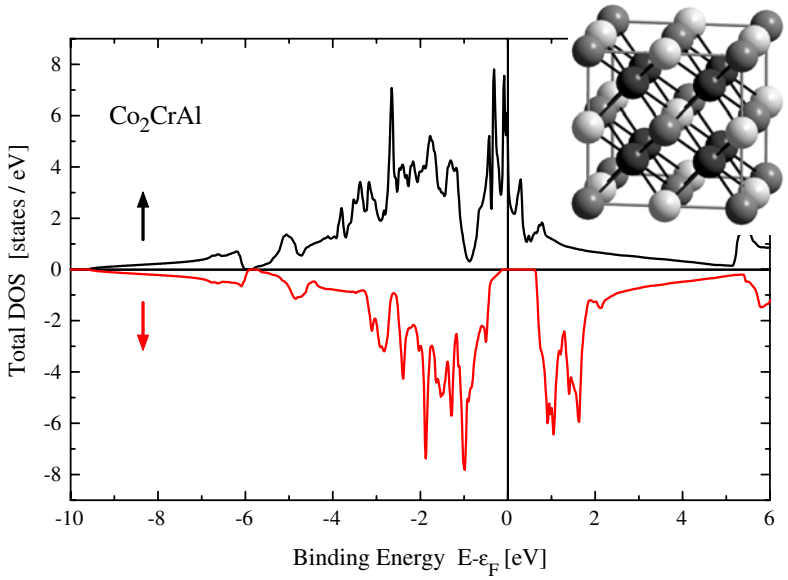

Figure 1. First principles calculation of the spin-resolved density of states of Co_2CrAl. The inset shows the $L2_1$ structure for a Heusler compound of the general formula X_2YZ. (X (dark grey), Y (medium grey) are transition metals and Z (light grey) a main group element. Exchange of Y and Z results in the same $L2_1$ structure.)

for large effects seems to be a high degree of spin polarization at the Fermi level. A group of special materials, the Heusler compounds, show particular features in their electronic structure that may cause a high magnetoresistance. Our band structure calculations predict that the ordered Heusler compound $Co_2Cr_{0.6}Fe_{0.4}Al$ should exhibit complete spin polarization at the Fermi level. The density of states reveals a half-metallic ferromagnet (HMF) with a van Hove singularity in the vicinity of the Fermi energy in the majority spin channel and a gap in the minority spin channel. Details of the calculation will be presented elsewhere [2].

Heusler compounds are of the general formula X_2YZ, where X and Y are usually transition metal elements and Z is a main group element, either a non-magnetic metal or a non-metal (see figure 1). Y may also be a rare earth element. The $L2_1$ crystal structure is marked by four interpenetrating fcc lattices. Ferromagnetic properties of Heusler compounds have been investigated experimentally and theoretically [3]. The Co-based Heusler compounds are of particular interest because they show comparatively high Curie temperatures.

For Co_2CrAl a ground state magnetic moment of 1.55 μ_B fu^{-1} (formula unit) has been reported by Buschow and van Engen [4] and it was considered that Co atoms mainly carry the magnetic moment in this material whereas the contribution of Cr and Al atoms remains small. Recent LMTO band structure calculations reveal a HMF character of the density of states, i.e. a gap at the Fermi level in the minority band and a high density of states in the majority band (see figure 1). According to our calculation all constituents of the compound should possess a magnetic moment, i.e. 0.77 μ_B/atom for Co, 1.63 μ_B/atom for Cr and -0.10 μ_B/atom for Al. For the total moment a value of approximately 3 μ_B fu^{-1} is obtained, in agreement with the rule of thumb for the magnetic moment, μ, of half-metallic Heusler compounds from 3d transition metals $\mu/\mu_B = N - 24$, with N being the cumulated number of valence electrons (4s, 3d for the 3d transition metals and 3s, 3p for Al). Reproducible magnetic moments can be obtained in agreement with the rule of thumb if Cr is partly replaced by Fe. According to band

structure calculations the electronic properties are mostly similar to those of Co_2CrAl. The replacement of Cr by Fe can be seen as a doping with electrons. Band structure calculations for the disordered variant confirm a strongly reduced magnetic moment (about 1 μ_B fu^{-1}) as well as a loss of the half-metallic character.

2. Experimental details

The ordered Heusler compound $Co_2Cr_{0.6}Fe_{0.4}Al$ was prepared by arc melting of the constituent elements under an argon atmosphere. The samples were cooled down to room temperature by rapidly shutting down the heating. Flat discs (8 mm diameter by 1 mm) were cut from the polycrystalline ingots and were mechanically polished. Neutron powder diffraction data for $Co_2Cr_{0.6}Fe_{0.4}Al$ revealed the well-ordered structure of a Heusler phase with a cubic lattice ($Fm\bar{3}m$) and a lattice constant of $a = 5.737$ Å. Using a SQUID magnetometer, we detected a saturation magnetic moment of 93 emu g^{-1} at $T = 6.5$ K and $B = 1$ T. The Curie temperature was determined as 760 K. The remanence of 2 emu g^{-1} and coercive field of 0.8 mT indicate that $Co_2Cr_{0.6}Fe_{0.4}Al$ is a soft magnet. This high magnetic moment corresponds to 3.25 ± 0.03 μ_B fu^{-1} (at room temperature) and is significantly reduced compared with the magnetic moment of 3.8 μ_B fu^{-1} predicted by the first principles band structure calculation. The reduction may be partly explained by the presence of paramagnetic clusters in the solid solution not visible via neutron diffraction but observable in the Mößbauer spectra [2]. Moreover, XMCD measurements [5] revealed a reduced Cr moment; see below.

First evidence for the predicted high magnetoresistance was found for $Co_2Cr_{0.6}Fe_{0.4}Al$ by measuring spin polarized transport at room temperature. In a small magnetic field of 0.1 T, we observed a relatively high powder magnetoresistance effect of up to 30% [2]. Figure 2 shows typical magnetoresistance curves of pressed powder compacts before and after annealing. Very recently, a large effect of 26% (at room temperature) was found for a tunnelling magnetoresistance element of the same compound [6].

We studied the chemical composition and homogeneity as well as the magnetic properties of the Heusler compound, particularly the behaviour of the magnetic domains and the element specific magnetic moments. The investigation focused on examining the suitability for magnetoelectronic applications. The experiments utilized photoelectron emission microscopy (PEEM) and x-ray magnetic circular dichroism (XMCD) at beamlines UE56/2-SGM and UE46-PGM of BESSY (Berlin, Germany) and XMCD at the First Dragon beamline of NSRRC (Hsinchu, Taiwan).

3. Results and discussion

The measurements were performed using circularly polarized synchrotron radiation at BESSY and a high-resolution photoelectron emission microscope (IS-PEEM, FOCUS GmbH). It magnifies the lateral photoelectron distribution from the sample surface generated by excitation with synchrotron radiation. A spatial resolution of about 100 nm can be reached with synchrotron-radiation excitation without aberration correction or energy analysis of the photoelectrons. Contrast of chemical, magnetic and topographic origin can be seen on the screen (for details of the method, see [7]).

In order to check whether the sample is chemically homogeneous, element-resolved images taken at the L_{III} edges of the corresponding elements as well as spatially resolved x-ray absorption spectroscopy (XAS) spectra are extracted by integrating over regions of interest. There are areas that show an enrichment of Cr at the expense of Fe and Co. The images 3(a)

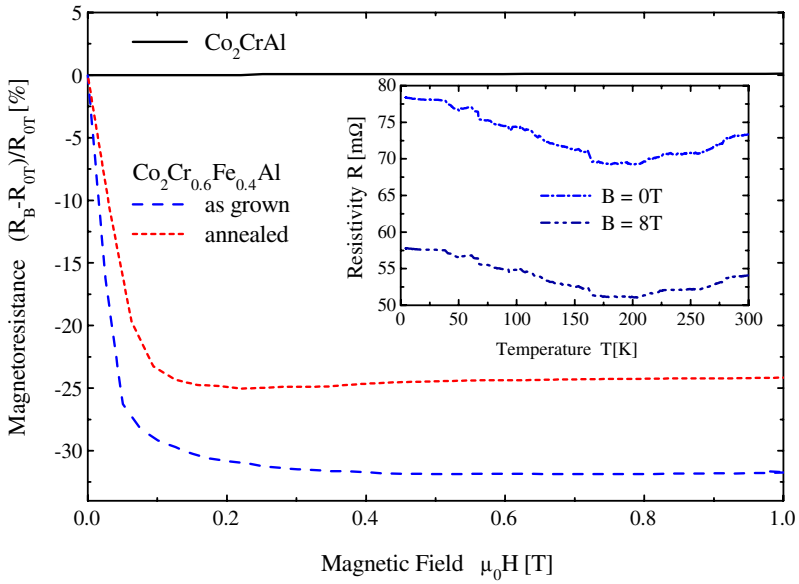

Figure 2. Magnetoresistance for $Co_2Cr_{0.6}Fe_{0.4}Al$ and Co_2CrAl at room temperature as a function of the external field. Co_2CrAl shows no detectable effect. Polycrystalline powder compacts show a large effect that decreases slightly upon annealing at 1300 K for 1 h. The inset shows the resistivity-versus-temperature curve of $Co_2Cr_{0.6}Fe_{0.4}Al$ at zero field and within an external field of 8 T.

and (b) were taken at the Cr and Co L_{II} edges, respectively. They show a needle shaped Cr rich area. Besides this local phase separation and some point-like defect structures the surface looks homogeneous in the element selective images thus giving evidence of a constant stoichiometry. The local XAS spectra in figure 3 were taken from the needle shaped defect and the flat surrounding area. They exhibit clearly a lack of Co and an increase of Cr at the defect. Similar spectra and images taken near and at the Fe L edges (not shown here) show a corresponding behaviour. A detailed analysis of the images and spectra taken in the energy range of the Cr L edges reveals that the oxidation state of the chromium is the same for the defect and the Heusler phase (see also below).

Magnetic contrast is obtained by either subtracting images for opposite photon helicities at either the L_{III} or L_{II} edge (circular dichroism) or those taken at the L_{III} and L_{II} edges at fixed photohelicity (magnetic dichroism). Figure 4 shows both types of asymmetry image (normalized difference). Comparison of the contrasts of the two types of asymmetry image allows one to distinguish the magnetic contrast from topographical or chemical effects.

Dark and bright areas in the circular dichroism images 4(a) and (b) correspond to magnetic domains with opposite magnetization and parallel to the projection of the photon beam. Domains with a mean grey value are aligned perpendicular to the photon beam. The images show the occurrence of micrometre-size domains. The ferromagnetic coupling between Fe and Co is clearly seen from the similar magnetic contrast measured at the L_{III} absorption edges of Fe and Co. On the sub-micrometre scale, a more complicated domain pattern (ripple structure) is resolved. At the Cr L edges no magnetic contrast exceeding the signal to noise level could be observed.

The Cr rich, needle shaped defects are still visible in the magnetic dichroism images of 4(c) and (d). Obviously, some part of the chemical information remains in this type of asymmetry that is not detectable in the circular dichroism images of 4(a) and (b).

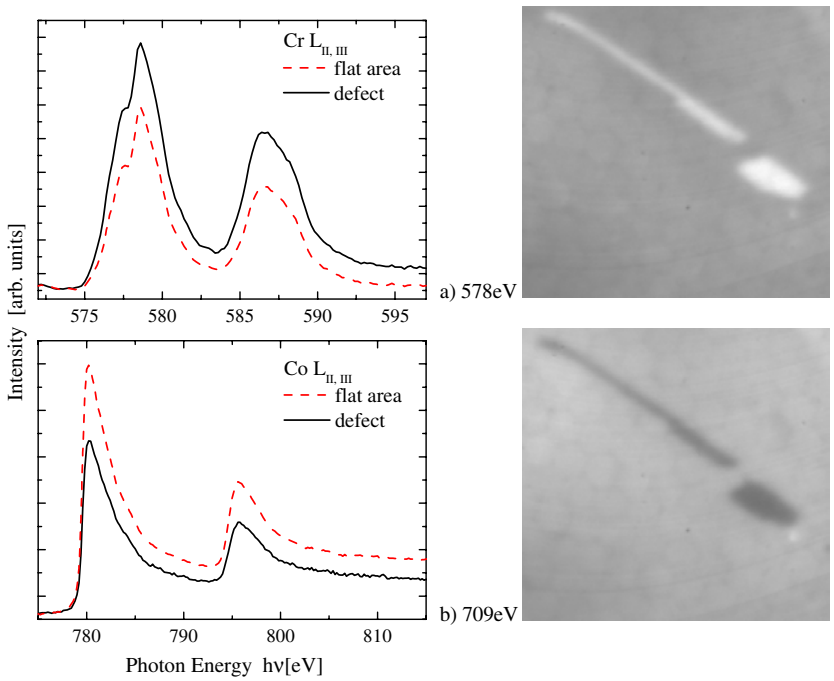

Figure 3. Element selective XAS-PEEM imaging of the $Co_2Cr_{0.6}Fe_{0.4}Al$ surface. The images (a) and (b) (size $4.6 \times 4.4\ \mu m^2$) and the local x-ray absorption spectra reveal a needle shaped Cr rich phase on a homogeneous background (Heusler phase).

The magnetic properties depend very sensitively on the stoichiometry. The surface was cleaned by Ar-ion bombardment for the present PEEM measurements. The magnetic contrast was very weak without cleaning. The micrometre-size magnetic domains, however, were still clearly present. The domain pattern reflects the properties of the Heusler compound although the Ar-ion bombardment did not fully remove the surface oxide layer as concluded from the XAS spectra. A thin oxide layer of about 1 nm may not change the domain pattern that is formed by the surface region of thickness similar to the domain size.

The observed domain structure is typical for non-oriented polycrystalline material [8]. It is caused by magnetostrictive interactions between adjacent grains. If magnetostriction along the easy axis is not zero, elastic interactions between the grains lead to additional conditions for the domain structure. The trend towards a homogeneous distribution of magnetoelastic and stray-field energy causes the *folded bands* [8] of basic domains as observed in figure 4. Magnetostrictive interactions also explain the surprisingly low magnetic remanence of less than 20% for our samples. Averaging over independent grains would lead to a remanence beyond 80% for cubic materials while magnetostrictive interactions can reduce the remanence considerably [8].

In order to investigate element specific magnetic properties and compare them with theoretical predictions, we have carried out measurements of the XMCD in the soft x-ray core-level absorption of Cr, Fe and Co in $Co_2Cr_{0.6}Fe_{0.4}Al$. XMCD in the $2p \rightarrow 3d$ transitions was measured at the First Dragon beamline at the NSRRC (Hsinchu, Taiwan) with a resolution of 80 meV at $h\nu = 800$ eV. The XAS spectrum was obtained by the total electron yield method, measuring directly the sample current while scanning the photon energy. The magnetic field applied to the sample (0.8 T) during the measurement was aligned with the surface normal and at

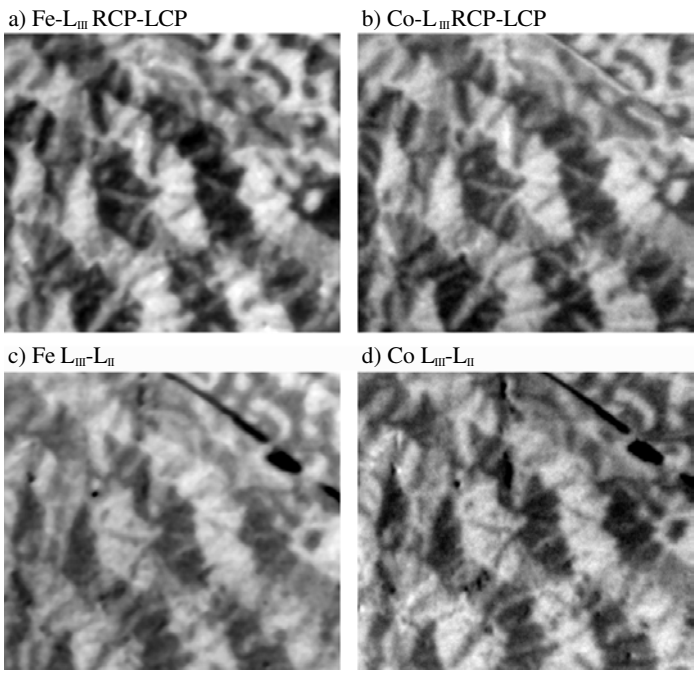

Figure 4. XMCD-PEEM images (size $9.3 \times 8.3\ \mu m^2$) revealing the micromagnetic domain contrast of $Co_2Cr_{0.6}Fe_{0.4}Al$. (a) and (b) show the circular dichroism at the L_{III} edges. Dark and bright areas correspond to magnetic domains with opposite magnetization and parallel to the projection of the photon beam. Domains with a mean grey value are aligned perpendicular to the photon beam. (c) and (d) show the magnetic dichroism at fixed helicity of the photons.

an angle of 30° with respect to the photon impact direction. The measurements revealed a strong selective oxidation of Cr when the polished sample surface was exposed to air. Consequently, the surfaces were scraped *in situ* in ultrahigh vacuum in order to remove the surface oxide layer (see figure 5).

A clear difference has been observed for the Cr XAS before and after removing the oxide layer. For clean surfaces, the XAS spectra look similar to spectra obtained from metallic Cr samples. Resonant absorption lines are obtained at 575.9 and 584.6 eV for the L_{III} and L_{II} edge, respectively, with a full width at half-maximum (FWHM) of about 3.5 eV, which is characteristic for Cr in the metallic state [9]. In contrast, the Cr XAS spectrum of the oxidized surface shows two distinct peaks at the L_{III} edge (575.9 and 577.0 eV) and the peak at the L_{II} edge is accompanied by a shoulder. The peak positions and relative intensities are characteristic for the XAS spectrum obtained from Cr_2O_3 [10].

The XAS spectra at the Fe L_{III} and L_{II} edges show resonant absorption lines at 707.7 and 721 eV, respectively, with a FWHM of about 2 eV; they are comparable to the XAS spectra of metallic Fe [11]. In particular, the oxidized sample does not show an additional peak at the Fe L_{III} edge, which could be expected for oxidized Fe at a photon energy shifted by 2 eV to higher binding energy [12].

As in the case of Fe, the XAS spectra at the Co L_{III} and L_{II} edges show two prominent resonant peaks at 778.6 and 793.8 eV, similarly to XAS spectra observed for metallic Co [11]. The FWHM is approximately 2 eV. No additional peaks can be recognized for the oxidized sample. In particular, no multiple peak structures in the L_{III} region were observed as in the case of the Sn-based Heusler compounds Co_2YSn (Y = Ti, Zr and Nb) [13]. The lack of

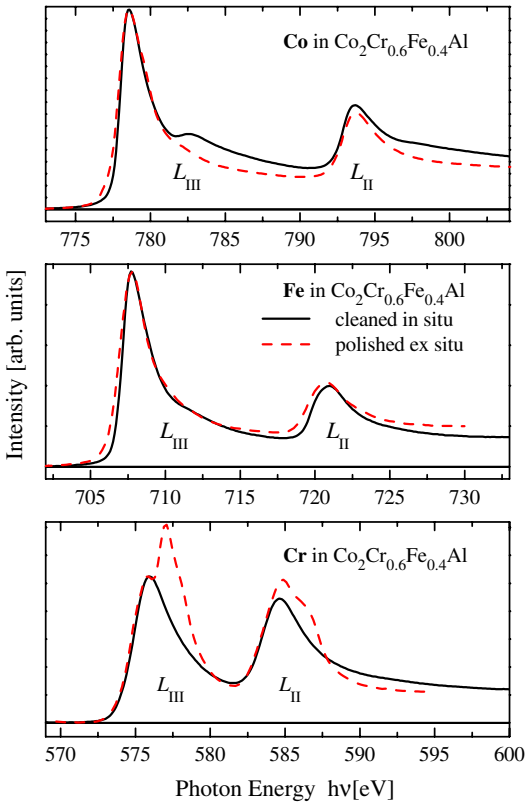

Figure 5. Cr, Fe and Co 2p → 3d4s XAS spectra for $Co_2Cr_{0.6}Fe_{0.4}Al$ before and after the *in situ* cleaning of the surface. The extra peaks at the Cr L_{III} and L_{II} adsorption edges of the as prepared sample indicate oxidized Cr, while the Fe and Co L_{III} and L_{II} adsorption edges show no oxide features. The extra peak at the Co L_{III} adsorption edge is caused by the particular band structure of the Heusler compound.

these multiple peak structures cannot be attributed to a limited energy resolution as can be concluded from the steep increase at 778 eV. Instead it must be explained by a different DOS which indicates a more metallic character of the Co d band as compared to the Co_2YSn alloys. For the quenched sample we observed a pronounced shoulder at the L_{III} peak shifted by 4 eV with respect to the maximum to a higher photon energy. A similar structure should be observed in the L_{II} region. A less pronounced shoulder can indeed be observed at the L_{II} peak. Less sharp structures in the L_{II} region can be attributed to a lifetime broadening effect because the lifetime of the $2p_{1/2}$ core hole is much shorter than that of the $2p_{3/2}$ core hole due to the Coster–Kronig decay [11].

Using the XMCD data (see figure 6) we have evaluated element specific magnetic moments by application of magneto-optical sum rules. Absolute values of spin and orbital moments were estimated using values of the total magnetic moments obtained by SQUID magnetometry. For quenched samples we obtained spin magnetic moments in agreement with the band structure calculations for Co and Fe atoms, whereas Cr possesses a reduced magnetic moment.

The orbital magnetic moments are $<10\%$ and $(11 \pm 2)\%$ of the spin moments for Cr and Co, respectively. The value for Cr may be seen as upper limit, as it depends strongly on the choice of the integration boundaries while performing the sum-rule analysis. For Fe the orbital moment is 7% of the spin moment, corresponding to an absolute value of $0.16 \pm 0.04\ \mu_B$,

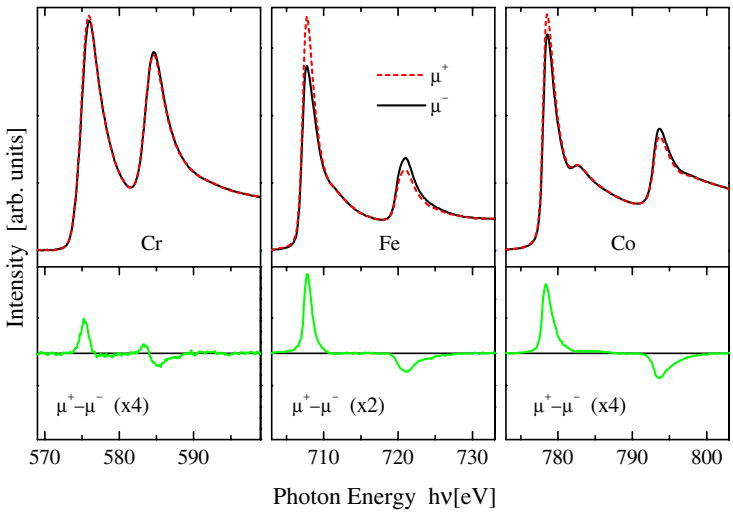

Figure 6. Cr, Fe and Co 2p → 3d XAS-MCD spectra for the quenched $Co_2Cr_{0.6}Fe_{0.4}Al$ compound. Solid (μ^-) and dashed (μ^+) curves show the XAS spectra measured with the external field applied parallel and antiparallel to the surface normal. The bottom panels represent the MXCD spectra (note the different scales).

which is considerably larger than the Fe bulk value (0.09 μ_B [5]). We attribute the origin of the large orbital moment of Fe to the localization of the Fe 3d electrons. The XMCD peak at the L_{III} edge of Fe turns out to be considerably narrower compared to the peak observed for bulk Fe. This observation supports the theoretical prediction of strongly localized 3d states. Annealing of $Co_2Cr_{0.6}Fe_{0.4}Al$ reduces the magnetic moments at Fe and Cr drastically. We tentatively attribute this to increased atomic disorder. Atomic disorder seems to play a major role for the magnetic properties of Heusler compounds.

From the comparison of the XAS spectra of oxidized samples with clean surfaces it is obvious that the three elements Cr, Fe and Co react differently when exposed to air. This can be expected, because the metal–oxygen bond enthalpy is larger for Cr (430 kJ mol^{-1}) than for Fe (400 kJ mol^{-1}) and Co (385 kJ mol^{-1}). The strong selectivity, however, is surprising. Cr is selectively oxidized whereas the majority of Co and Fe remains in a metallic state. The information depth of XAS involves a surface layer of 1.2 nm thickness, i.e. 2–4 unit cells. Therefore, the selective oxidation of Cr involves a surface segregation process, which at least partially destroys the stoichiometry of these Heusler compounds in the surface region. Taking this into account, one may conclude that the near surface region of about 1.2 nm consists of a metallic FeCo alloy mixed by Cr oxide, after exposure to air. From its chemical reactivity (Al–O bond enthalpy 511 kJ mol^{-1}) one might assume that Al is oxidized as well. The selective segregation of Cr to the grain boundaries is known for other magnetic materials [14] and is utilized for a magnetic decoupling of adjacent grains in high-data-density magnetic storage media.

4. Conclusions

We have measured the XMCD in Cr, Fe and Co 2p → 3d XAS of the ferromagnetic Heusler compound $Co_2Cr_{0.6}Fe_{0.4}Al$. We observed a strong selective oxidation of Cr when polished surfaces were exposed to air, involving a change of electronic properties at the surface. The different properties of the surface compared to the bulk have to be taken into account for the

interpretation of magnetoresistance effects in powder compacts [2, 15–17] with respect to a potentially high spin polarization of the Heusler compounds. Surface properties of the Heusler compounds may be important for the observed significant decrease of the magnetoresistance in pressed powders [2]. It may also influence the verification of a total spin polarization by means of Andreev reflections [18]. A selective oxidation at the surface could potentially lead to a misinterpretation of the results using the latter method.

Element specific magnetic moments have been determined using magneto-optical sum rules. Absolute values of spin and orbital magnetic moments were estimated using values of the total magnetic moment obtained by SQUID magnetometry. For quenched samples we obtained spin magnetic moments in agreement with band structure calculations for Co and Fe atoms whereas Cr atoms possess a reduced magnetic moment. Orbital magnetic moments are between 10% and 14% of the spin moment. The value for Fe corresponds to an absolute value of 0.16 μ_B which is considerably larger than the Fe bulk value. We attribute the origin of the large orbital moment of Fe as the localization of the Fe 3d electrons. Annealing of $Co_2Cr_{0.6}Fe_{0.4}Al$ reduces magnetic moments at Fe and Cr drastically which we tentatively attribute to an increased atomic disorder. Atomic disorder seems to play a major role for the magnetic properties of Heusler compounds.

Domain imaging via MXCD-PEEM and element specific magnetometry in combination with theoretical band structure calculations provides a key tool for understanding the influence of disorder and of the particular electronic properties of Heusler alloys. A careful preparation of the surface is necessary due to the selective oxidation.

Acknowledgments

The authors thank all members of BESSY (Berlin, Germany) and NSRRC (Hsinchu, Taiwan) for their help during the beamtimes. We thank P-C Hsu and W-L Tsai for help with the experiments. GHF and SW are very grateful to Y Hwu (Academia Sinica, Taipei) and H-M Lin (Tatung University, Taipei) for their support during the experiments in Taiwan.

References

[1] Prinz G A 1998 *Science* **282** 1660
[2] Block T, Felser C, Jakob G, Ensling J, Mühling B, Gütlich P, Beaumont V, Studer F and Cava R J 2003 *J. Solid State Chem.* at press
[3] Webster P J 1971 *J. Phys. Chem. Solids* **32** 1221
[4] Buschow K H J and van Engen P G 1981 *J. Magn. Magn. Mater.* **25** 90
[5] Elmers H J, Fecher G H, Valdaitsev D, Nepijko S A, Gloskovskii A, Jakob G, Schönhense G, Wurmehl S, Block T, Felser C, Hsu P-C, Tsai W L and Cramm S 2003 *Phys. Rev.* B **67** 104412
[6] Inomata K, Okamura S, Goto R and Tezuka N 2003 *Japan. J. Appl. Phys.* **42** L419
[7] Schneider C M and Schönhense G 2002 *Rep. Prog. Phys.* **65** R1785
[8] Hubert A and Schäfer R 1998 *Magnetic Domains* (Berlin: Springer) pp 532–8
[9] Tomaz M A, Antel W J, O'Brien W L and Harp G R 1997 *Phys. Rev.* B **55** 3716
[10] Theil C, van Elp J and Folkmann F 1999 *Phys. Rev.* B **59** 7931
[11] Shen C T, Idzerda Y U, Lin H-J, Smith N V, Meigs G, Chaban E, Ho G H, Pellegrin E and Sette F 1995 *Phys. Rev. Lett.* **75** 152
[12] Hochepied J F, Sainctavit Ph and Pileni M P 2001 *J. Magn. Magn. Mater.* **231** 315
[13] Yamasaki A, Imada S, Arai R, Utsunomiya H, Suga S, Muro T, Saitoh Y, Kanomata T and Ishida S 2002 *Phys. Rev.* B **65** 104410
[14] Hono K, Okano R, Takanashi K, Fujimori H, Maeda Y and Sakurai T 1995 *MRS Symp. Proc.* **384** 507
[15] Gupta A and Sun J Z 1999 *J. Magn. Magn. Mater.* **200** 24
[16] Coey J M D, Berkowitz A E, Balcells L, Putris F F and Barry A 1998 *Phys. Rev. Lett.* **80** 3815
[17] Soulen R J Jr, Byers J M, Osofsky M S, Nadgorny B, Ambrose T, Cheng S F, Broussard P R, Tanaka C T, Nowak J, Moodera J S, Barry A and Coey J M D 1998 *Science* **282** 85
[18] Auth N, Jakob G, Block T and Felser C 2003 *Phys. Rev.* B **68** 024403